Bexotegrast Shows Dose-dependent Integrin $\alpha_v\beta_6$ Receptor Occupancy in Lungs of Participants with Idiopathic Pulmonary Fibrosis: A Phase 2, Open-Label Clinical Trial

Joshua J. Mooney,[1] Susan Jacobs,[1] Éric A. Lefebvre,[2] Gregory P. Cosgrove,[2] Annie Clark,[2] Scott M. Turner,[3] Martin Decaris,[2] Chris N. Barnes,[2] Marzena Jurek,[3] Brittney Williams,[4] Heying Duan,[4] Richard Kimura,[4] Gaia Rizzo,[5] Graham Searle,[5] Mirwais Wardak,[4] H. Henry Guo[4]

[1]Department of Medicine, Division of Pulmonary, Allergy and Critical Care, Stanford University, Stanford, CA, USA; [2]Pliant Therapeutics, Inc., South San Francisco, CA, USA; [3]Former employee of Pliant Therapeutics, Inc., South San Francisco, CA, USA; [4]Department of Radiology, Nuclear Medicine and Molecular Imaging Division, Stanford University, Stanford, CA, USA; [5]Former employee of Invicro, London, UK

Corresponding author:

H. Henry Guo, MD, PhD

Stanford University

Department of Radiology

435 Quarry Rd

Palo Alto, CA 94304

henryguo@stanford.edu

Telephone: (650) 736-9909

Fax: (650) 725-7296

ANNALSATS Articles in Press. Published November 05, 2024 as 10.1513/AnnalsATS.202409-969OC

Author contributions

All authors contributed to, reviewed, and approved the final draft of the paper. All authors had full access to all the data in the study and had final responsibility for the decision to submit for publication.

Concept and design: JJM, EAL, GPC, SMT, MD

Development and validation of the PET tracer: JJM, RK, HHG

Acquisition, analysis, or interpretation of data: JJM, EAL, GPC, AC, SMT, MD, CNB, HD, GR, GS, MW

Drafting of manuscript: all authors

Critical revision of the manuscript for important intellectual content: all authors

Statistical analysis: CNB

Funding: This study was sponsored by Pliant Therapeutics, Inc. Editorial assistance was provided by Richard Karpowicz, PhD, CMPP, of Nucleus Global, Inc., and was funded by Pliant Therapeutics, Inc.

Short title (50 characters maximum, including spaces; current: 45): Imaging Bexotegrast Receptor Occupancy in IPF

Journal descriptor number: 9.23 Interstitial Lung Disease

Keywords (3-5 max): IPF, PET imaging, fibrotic disease, investigational treatment, safety

Word count: 3500 words maximum; current: **3487**

ANNALSATS Articles in Press. Published November 05, 2024 as 10.1513/AnnalsATS.202409-969OC

This article has an online data supplement, which is accessible at the Supplements tab.

Clinical trial registration available at www.clinicaltrials.gov, ID: NCT04072315.

ANNALSATS Articles in Press. Published November 05, 2024 as 10.1513/AnnalsATS.202409-969OC

Abstract

Rationale: Idiopathic pulmonary fibrosis (IPF) is a chronic and progressive disease characterized by dyspnea and loss of lung function. Transforming growth factor-beta (TGF-β) activation mediated by α_v integrins is central to the pathogenesis of IPF. Bexotegrast (PLN-74809) is an oral, once-daily, dual-selective inhibitor of $\alpha_v\beta_6$ and $\alpha_v\beta_1$ integrins under investigation for the treatment of IPF. Positron emission tomography (PET) using an $\alpha_v\beta_6$-specific PET tracer could confirm target engagement of bexotegrast in the lungs of participants with IPF.

Objectives: This Phase 2 study (NCT04072315) evaluated $\alpha_v\beta_6$ receptor occupancy in the lung, as assessed by changes from baseline in $\alpha_v\beta_6$ PET tracer uptake, following single dose administration of bexotegrast to participants with IPF.

Methods: In this open-label, single-center, single-arm study, adults with IPF received up to 2 single doses of bexotegrast, ranging from 60 to 320 mg with or without background IPF therapy (pirfenidone or nintedanib). At baseline and approximately 4 hours after each orally administered bexotegrast dose, a 60-minute dynamic PET/CT scan was conducted following administration of an $\alpha_v\beta_6$-specific PET probe ([^{18}F]FP-$R_0$1-MG-F2). $\alpha_v\beta_6$ receptor occupancy by bexotegrast was estimated from the changes in PET tracer uptake following bexotegrast. Pharmacokinetics, safety, and tolerability of bexotegrast were also assessed.

Results: Eight participants completed the study. Total and unbound plasma bexotegrast concentrations increased in a dose-dependent manner, and regional PET volume of distribution (V_T) values decreased in a dose- and concentration-dependent manner. The V_T data fit a simple saturation model, producing an unbound bexotegrast EC_{50} estimate of 3.32 ng/mL. Estimated maximum receptor occupancy was 35%, 53%, 71%, 88%, and 92% following single 60, 80, 120, 240, and 320-mg

ANNALSATS Articles in Press. Published November 05, 2024 as 10.1513/AnnalsATS.202409-969OC

doses of bexotegrast, respectively. No treatment-emergent adverse events related to bexotegrast were reported.

Conclusions: Dose- and concentration-dependent $\alpha_v\beta_6$ receptor occupancy by bexotegrast was observed by PET imaging, supporting once-daily 160 to 320 mg dosing to evaluate efficacy in clinical trials of IPF.

Trial registration number: NCT04072315

Primary source of funding: Pliant Therapeutics, Inc.

Abstract word count: 350 words max; **current: 310**

ANNALSATS Articles in Press. Published November 05, 2024 as 10.1513/AnnalsATS.202409-969OC

INTRODUCTION

Idiopathic pulmonary fibrosis (IPF) is a chronic, progressive form of fibrotic interstitial lung disease of unknown cause (1, 2). IPF is characterized by cough and dyspnea resulting from scarring of the lungs due to excessive extracellular matrix deposition (1, 3-5). The prognosis of patients with IPF is poor, with a median life expectancy of approximately 3 to 4 years after diagnosis (6, 7).

Transforming growth factor-beta (TGF-β) signaling activated by α_v integrins is a key driver of fibrosis in the lungs (8-10). Increased expression of integrins $\alpha_v\beta_6$ on lung epithelial cells and $\alpha_v\beta_1$ on lung fibroblasts activates latent TGF-β (10-13), resulting in SMAD2/3 phosphorylation, profibrotic gene expression, and resultant collagen deposition in the lungs (8, 12, 14). Elevated levels of integrins $\alpha_v\beta_6$ and $\alpha_v\beta_1$ are detectable in the lungs of patients with IPF compared with healthy people (12, 15, 16). High levels of integrin $\alpha_v\beta_6$ detected within lung tissue biopsies (17) and plasma (18, 19) are also predictors of worse survival rates for patients with IPF.

TGF-β is involved in multiple different biological functions, and its systemic inhibition can lead to significant safety concerns; as such, there is a need for IPF therapies that inhibit TGF-β signaling specifically at the site of fibrosis (20, 21). Since $\alpha_v\beta_6$ and $\alpha_v\beta_1$ expression levels closely accompany lung injury and fibrogenesis (10, 13), it is proposed that dual-selective inhibition of the $\alpha_v\beta_6/\alpha_v\beta_1$-TGF-β axis may allow for a localized, and therefore potentially safer, approach to reducing TGF-β activation in the fibrotic lung.

Bexotegrast (PLN-74809) is an oral, once-daily, dual-selective inhibitor of $\alpha_v\beta_6$ and $\alpha_v\beta_1$ integrins in development for the treatment of IPF (12). In a Phase 2 study of participants with IPF, bexotegrast showed a favorable safety profile up to 40 weeks of treatment, and showed improved lung function and antifibrotic effects based on

ANNALSATS Articles in Press. Published November 05, 2024 as 10.1513/AnnalsATS.202409-969OC

forced vital capacity (FVC), quantitative lung fibrosis imaging, and circulating levels of plasma integrin beta 6 (ITGB6) and serum type III collagen synthesis neoepitope (PRO-C3) (22).

An $\alpha_v\beta_6$ cystine knot peptide radiotracer known as the Knottin tracer, [^{18}F]FP-$R_0$1-MG-F2, binds specifically to $\alpha_v\beta_6$ and has been used to detect increased $\alpha_v\beta_6$ expression by PET in the lungs of patients with IPF (15). Non-invasive imaging studies of bexotegrast binding to $\alpha_v\beta_6$ in fibrotic lungs using this tracer could assist in dose selection in future studies, verify access to integrin targets with orally bioavailable agents in the architecturally distorted parenchyma with aberrant pulmonary vasculature in fibrotic lung, and contribute to a comprehensive understanding of receptor occupancy in IPF.

The objective of this Phase 2 study was to evaluate $\alpha_v\beta_6$ receptor occupancy by bexotegrast in the lungs of participants with IPF, as assessed by changes from baseline in $\alpha_v\beta_6$ PET tracer uptake following a single dose of bexotegrast. Safety, tolerability, and pharmacokinetics (PK) of bexotegrast were also explored. Our hypothesis was that bexotegrast and the [^{18}F]FP-$R_0$1-MG-F2 radiotracer bind to the same target in the fibrotic lung and that PET imaging with this radiotracer will non-invasively visualize disease-related receptors and quantify receptor occupancy by bexotegrast in participants with IPF. A portion of the results of these studies have been previously published in the form of abstracts (23, 24).

METHODS

Study population

This Phase 2, open-label, single-site study (NCT04072315) was conducted at Stanford University in Stanford, CA, USA. The study enrolled participants aged ≥40

ANNALSATS Articles in Press. Published November 05, 2024 as 10.1513/AnnalsATS.202409-969OC

years with a diagnosis of IPF within 8 years prior to screening, according to the Fleischner Society White Paper criteria (25), with high-resolution computed tomography (CT) imaging showing a typical or probable usual interstitial pneumonia pattern, FVC percent predicted ≥45%, and diffusing capacity of the lungs for carbon monoxide (DL_{CO}) adjusted for hemoglobin values ≥30%. Background therapy for IPF with pirfenidone or nintedanib was permitted, provided these drugs had been given at a stable dose for ≥3 months prior to screening. Key exclusion criteria included receiving any non-approved agent intended for the treatment of pulmonary fibrosis or IPF, the presence of airway obstruction (ratio <0.7 for forced expiratory volume during the first second divided by FVC), and known acute IPF exacerbation or suspicion of such within 6 months of screening.

All eligible participants were enrolled in the study and included in the intention to treat (ITT) population. All participants who received at least 1 dose of bexotegrast were included in the safety population. All dosed participants with a baseline PET scan and ≥1 post-baseline PET scan were included in the modified ITT (mITT) population. The mITT population was used to assess the primary objective of the study. All participants who received ≥1 dose of bexotegrast and had any measurable bexotegrast concentration data were included in the PK concentration population, and all participants who had sufficient bexotegrast concentration data for PK calculation were included in the PK analysis population.

Study design

All participants received up to 2 single oral doses of bexotegrast, as a 60-mg oral solution or as an 80-mg, 120-mg, 240-mg, or 320-mg tablet formulation. The planned bexotegrast single doses for this study were selected to approximate steady-state

ANNALSATS Articles in Press. Published November 05, 2024 as 10.1513/AnnalsATS.202409-969OC

concentrations achieved by daily doses in the Phase 2 INTEGRIS-IPF study (PLN-74809-IPF-202; NCT04396756) (22).

Participants underwent dynamic PET scans for 60 minutes at baseline (Day −7) and on the day of bexotegrast dosing (Day 1) (**Figure 1**) after administration of [^{18}F]FP-R$_0$1-MG-F2, to evaluate $\alpha_v\beta_6$ receptor occupancy by bexotegrast. Participants were injected with 277.5 MBq (7.5 mCi ± 20%) of [^{18}F]FP-R$_0$1-MG-F2. Post-dose imaging for the assessment of $\alpha_v\beta_6$ receptor occupancy was performed to coincide with the anticipated time-to-maximum-observed bexotegrast concentration, approximately 4 hours after administration. PET data were assessed using tracer kinetic models described below to determine the total volume of distribution (V_T) in regions of interest (ROIs) within the lung.

Following a ≥14-day washout period, participants could receive a second single bexotegrast dose at a different dose level. If a participant received 2 single doses, only 1 baseline pre-dose PET scan was obtained. No more than 3 PET scans (baseline + 1 or 2 dosing scans) were obtained for any participant.

This study was conducted in accordance with the study protocol, the Declaration of Helsinki, and the International Council on Harmonisation Good Clinical Practice regulations. The study was approved by the institutional review board. All participants provided written informed consent.

Study objectives

The primary objective was to evaluate $\alpha_v\beta_6$ receptor occupancy by bexotegrast as assessed by changes from baseline in [^{18}F]FP-R$_0$1-MG-F2 radiotracer uptake in the lung following a single dose of bexotegrast. Secondary objectives included the assessment of safety and tolerability of bexotegrast in participants, as assessed by

ANNALSATS Articles in Press. Published November 05, 2024 as 10.1513/AnnalsATS.202409-969OC

incidence and severity of treatment-emergent adverse events (TEAEs), as well as clinical safety laboratory measures, vital signs, and electrocardiogram measures. Exploratory endpoints included evaluating the relationship between bexotegrast plasma concentration and PET imaging parameters, changes in V_T from baseline following single doses of bexotegrast, and determination of the unbound plasma concentration of bexotegrast that corresponds to 50% of maximal change in V_T (EC_{50}).

PK assessments

Bexotegrast plasma PK samples were obtained pre dose and at 0.5, 1, 2, 3, 4, and 24 hours post dose for determination of total and unbound bexotegrast concentrations. Details of PK assessments can be found in the **Supplemental Methods**.

Image and data analysis

PET image processing was performed using Invicro's VivoQuant software (v2020). PET data modeling was performed using Invicro's in-house MIAKAT™ software package (version 4.3.25). MIAKAT™ is implemented using MATLAB R2022a (The Mathworks Inc., Natick, MA, USA).

ROIs selected for image processing included the lungs, cardiac blood pool, and erector spinae muscle. The muscle ROI was defined as the reference region. Blood pool and lung ROIs were used for modeling and analysis. The muscle and cardiac blood pool regions were delineated using fixed spheres of radius 4 and 5 voxels, respectively, in Invicro's VivoQuant software. Spheres were placed manually using the CT scan for anatomical reference. A semi-automated method using custom

ANNALSATS Articles in Press. Published November 05, 2024 as 10.1513/AnnalsATS.202409-969OC

MATLAB scripts was used for segmenting the lung ROIs. Preliminary segmentation began by isolating the body in the image from the bed and background. The lungs were then identified as the largest connected component of low attenuation voxels in the body. Morphological open and close operations were used to capture higher attenuation tissue in the lungs. A final quality control including manual review and editing was performed to complete the lung segmentations. The segmentation derived from the CT scan was then applied to the PET image to generate time-activity curves (TACs), normalized in standardized uptake value, calculated as radioactivity concentration (kBq/cm^3) / (radioactivity injected [MBq] / body weight [kg]). The top 25th percentile of lung signal at 60 minutes was automatically identified and segmented into a separate ROI (lung25). The lung25 and whole lungs ROIs were used in the modeling and analysis.

Arterial blood data processing

The cardiac blood pool region, defined as the tracer radioactivity in the heart, was used to derive an input function for the kinetic models, assuming no metabolism of the tracer and equal tracer concentration in plasma and whole blood. The blood TAC was smoothed post peak using a tri-exponential fit to give the required blood input function. The resulting blood input function was used as input for the kinetic modeling processes described below.

Kinetic modeling

The derived tissue TACs were analyzed using the 1- and 2-tissue compartment (1TC, 2TC) models for reversible binding, with fitted blood volume component (26). The aim of the kinetic modeling process was to generate regional estimates of the

ANNALSATS Articles in Press. Published November 05, 2024 as 10.1513/AnnalsATS.202409-969OC

PET V_T. The most appropriate model was selected as a balance between model parsimony and goodness-of-fit, assessed via visual inspection of model fits to tissue TACs and parameters such as the Akaike information criterion and the coefficients of variation associated with estimated V_T values. V_T values were calculated for each participant, scan, and ROI.

Signal change evaluation

For each participant, the change in tracer uptake after the administration of bexotegrast was calculated from the regional V_T estimates to derive a ΔV_T for each post-dose scan (and ROI) as Equation 1:

$$\Delta V_T(\%) = 100\left(\frac{V_{T_{baseline}} - V_{T_{post\ dose}}}{V_{T_{baseline}}}\right) \quad (1)$$

where $V_{T_{baseline}}$ and $V_{T_{post\ dose}}$ are the V_T values calculated for the baseline and the post-dose scan, respectively. The muscle ROI was included to assess its potential utility as a reference region.

Analysis of the PK-V_T relationship

The PK-V_T relationship in the study population was explored by plotting the V_T values in lungs against the concentration of unbound bexotegrast in plasma at the time of the PET scan for all scans and participants. These data were fitted with Equation 2:

$$V_T = V_{ND} + V_s\left(1 - \frac{C_p}{C_p + EC_{50}}\right) \quad (2)$$

where V_{ND} is the non-displaceable volume of distribution, V_S is the specific volume of distribution, Cp is the (measured) unbound concentration in plasma of bexotegrast, and EC_{50} is the plasma concentration of bexotegrast that corresponds to 50%

ANNALSATS Articles in Press. Published November 05, 2024 as 10.1513/AnnalsATS.202409-969OC

maximal signal change at the time point being studied. Once an estimate of EC_{50} was obtained, estimates of EC_{80} and EC_{90} were calculated using Equation 3:

$$EC_X = EC_{50}\frac{X}{100-X} \quad (3)$$

where X is the percentage of maximal effect and EC_X is the plasma concentration of bexotegrast that corresponds to an effect of X%. For illustrative purposes, a plot of peak effect E (as a percentage of maximal effect) against unbound plasma concentration of bexotegrast was also produced, using Equation 4:

$$E(\%) = 100\frac{C_p}{C_p+EC_{50}} \quad (4)$$

Statistical analysis

The primary endpoint, change in PET V_T, was summarized using the kinetic modelling as described previously. PK and laboratory data were summarized using standard descriptive statistics. Adverse events data were summarized using the count and proportion of participants.

RESULTS

Study participants

Participant disposition is reported in **Figure 2**. A total of 11 participants underwent screening and were enrolled. Eight participants (72.7%) completed the study, and 3 participants (27.3%) withdrew prematurely, 2 prior to bexotegrast dosing (1 each for administrative reasons and withdrawn consent by participant) and 1 after bexotegrast administration.

At baseline, most participants were male, and the mean (SD) age was 77.6 (4.4) years (**Table 1**). Overall, 7 participants (77.7%) were receiving nintedanib and 1 participant (11.1%) was receiving pirfenidone as background therapy during the study.

ANNALSATS Articles in Press. Published November 05, 2024 as 10.1513/AnnalsATS.202409-969OC

PK assessments

Mean total and unbound plasma bexotegrast concentration-time profiles are presented in **Figure 3**, indicating dose-dependent increases in plasma bexotegrast concentration. Median time to maximum observed plasma concentration ranged from approximately 2 hours (60 mg) to 3.5 hours (240 mg).

PET imaging data

The baseline PET scan and at least 1 post-baseline PET scan were quantified for 8 study participants (60 mg, n=1; 80mg, n=2; 120 mg, n=3; 240 mg, n=3; 320 mg, n=4). Images showed heterogenous PET tracer signal in the lung tissue. Example baseline PET, CT, and overlaid PET/CT images demonstrating increased PET tracer uptake in areas of fibrosis are shown in **Figure E1**. Example regional TACs are shown in **Figure E2**. In whole lungs and lung25 ROIs, there was typically an early peak within the first few minutes of the tracer injection, representing distribution of the radiolabeled tracer, primarily in the blood volume component of the tissue. This was followed by a period with slower kinetics and markedly higher signal in the lung25 ROI than the whole lungs, indicating significant heterogeneity within the lungs. Muscle TACs were generally lower and slower than lung TACs.

Kinetic modeling

Both PET kinetic models (1TC and 2TC) produced visually acceptable model fits to the tissue TACs. As V_T values from both models were similar and highly correlated, the simpler 1TC model was selected as most appropriate. **Figure E3** shows an example of tissue TACs and corresponding 1TC model fits. For baseline scans, the

ANNALSATS Articles in Press. Published November 05, 2024 as 10.1513/AnnalsATS.202409-969OC

V_T estimates for the lung25 ROI were markedly higher (mean [SD]: 2.43 [0.909] mL/cm^3; range: 1.14–3.82 mL/cm^3) than for the whole lungs (mean [SD]: 1.42 [0.639] mL/cm^3; range: 0.57–2.73 mL/cm^3) or muscle (mean [SD]: 1.22 [0.500] mL/cm^3; range: 0.67–2.00 mL/cm^3).

Signal change evaluation upon bexotegrast treatment

V_T values generally decreased from baseline following administration of bexotegrast. For all participants, the lung25 ROI showed a dose-dependent decrease in V_T (**Figure 4**). This decrease was observed in the whole lungs and muscle ROIs as well. Since the V_T values for the muscle ROI consistently decreased from baseline after administration of bexotegrast, its use as a potential reference region was not explored further. Relative decreases in V_T (ΔV_T) were calculated using Equation 1 for lung25 and the magnitude generally increased in a dose-dependent manner (range of ΔV_T [%]: bexotegrast 60 mg, 41.0%; 80 mg, 2.0% to 41.5%; 120 mg, 33.3% to 61.4%; 240 mg, 44.6% to 61.0%; 320 mg, 24.3% to 64.8%).

Analysis of the PK-V_T relationship

PET scans were commenced approximately 4 hours after administration of bexotegrast. PK data were available for the nominal 4-hour time point for 12 of the 13 post-dose scans. The 3-hour time point was used in place of the missing 4-hour time point for 1 scan.

V_T values for the lung25 ROI are plotted against unbound plasma concentration values in **Figure 5**. Model fit parameters estimated by fitting Equation 2 to the PK and V_T data together are shown in **Table 2**. The estimated EC_{50} for the lung25 ROI was 3.32 ng/mL (95% CI, −4.19 to 10.83 ng/mL), corresponding via

ANNALSATS Articles in Press. Published November 05, 2024 as 10.1513/AnnalsATS.202409-969OC

Equation 3 to an EC_{80} of approximately 13.3 ng/mL and an EC_{90} of approximately 29.9 ng/mL.

Receptor occupancy of $\alpha_v\beta_6$ by bexotegrast, suggested by treatment-induced changes in V_T, was observed to be dose and concentration dependent, with estimated mean (range) maximum receptor occupancy of 35% (n=1), 53% (37%-63%), 71% (62%-83%), 88% (64%-94%), and 92% (83%-96%) following administration of single doses of 60, 80, 120, 240, and 320 mg bexotegrast, respectively (**Figure 6**). Representative PET images at baseline and after administration of bexotegrast 320 mg are shown in **Figure 7**. Bexotegrast doses ≥80 mg resulted in peak mean unbound concentrations above the estimated EC_{50} (**Table E1**).

Safety

No serious TEAEs were reported, and no participant experienced a TEAE that was related to study drug (**Table E2**). One participant (who received a single dose of bexotegrast 320 mg) experienced TEAEs on treatment. These were moderate (Grade 2) TEAEs of hepatic enzyme increase and gamma-glutamyl transferase increase on Day 2 that led to withdrawal from the study on Day 8 and were deemed not related to the study drug. The participant had a medical history of hyperbilirubinemia, which was considered an alternative causality. This participant was concomitantly receiving nintedanib for treatment of IPF, with known adverse reactions of liver enzyme elevations (27), and nintedanib dosing was stopped on Day 8. Hematology, clinical chemistry, urinalysis, physical examination findings, and vital sign parameters remained stable over time, and there were no clinically significant

ANNALSATS Articles in Press. Published November 05, 2024 as 10.1513/AnnalsATS.202409-969OC

echocardiogram changes during the treatment period. No deaths occurred during the study.

DISCUSSION

There exists an unmet medical need for a safe treatment capable of inhibiting and potentially reversing fibrosis in the lungs of patients with IPF. Currently available IPF therapies, nintedanib and pirfenidone, reduce the decline of lung function and potentially improve survival with continuous treatment (28-32). However, these drugs do not inhibit the progression of IPF, and they do not consistently improve patients' quality of life (30, 32). The tolerability of these 2 agents also remains a challenge, resulting in some patients with IPF patients having to discontinue treatment or undergo dose reductions (33).

Although TGF-β signaling is an attractive target for IPF drug development, safety concerns associated with systemic TGF-β inhibition highlight the need for specificity within fibrotic tissue. Localized TGF-β inhibition in the fibrotic lung, achieved by inhibiting $\alpha_v\beta_6$ and $\alpha_v\beta_1$ integrins with bexotegrast, may provide a novel approach for treating IPF without affecting TGF-β signaling systemically.

In the current study, the dose and exposure response of bexotegrast with $\alpha_v\beta_6$ integrin was investigated by performing PET imaging with a competitive $\alpha_v\beta_6$-binding probe, [^{18}F]FP-$R_0$1-MG-F2 (15), at or near the maximum observed concentration of bexotegrast (a plain language infographic is provided in the Online Data Supplement). V_T values in the lung25 and whole lung ROIs decreased in a dose- and concentration-dependent manner, consistent with bexotegrast binding to $\alpha_v\beta_6$ integrin in the lungs, suggesting that doses between 120 mg and 320 mg may provide optimal receptor occupancy and providing further support for the 160 mg and

ANNALSATS Articles in Press. Published November 05, 2024 as 10.1513/AnnalsATS.202409-969OC

320 mg doses currently evaluated in the ongoing Phase 2b/3 BEACON-IPF study (NCT06097260). No corrections for air volume fraction were made, so the signal in lungs per-unit-volume of solid tissue may be more elevated relative to other tissues than the V_T values suggest. These results support receptor occupancy of bexotegrast to $\alpha_v\beta_6$ integrin present in fibrotic tissue in the lungs of participants with IPF. While not directly assessed in the current study, we anticipate a similar rate of receptor occupancy for $\alpha_v\beta_1$ integrins, given the IC_{50} of bexotegrast is roughly equipotent for $\alpha_v\beta_1$ and $\alpha_v\beta_6$ integrins in both ligand binding and TGF-β activation assays (12). Bexotegrast was well tolerated at the doses administered in the current study, with no participants experiencing serious TEAEs or TEAEs related to bexotegrast treatment.

In a previous Phase 1 study in participants with IPF that included PET imaging with an $\alpha_v\beta_6$-specific PET ligand [^{18}F]FB-A20FMDV2, $\alpha_v\beta_6$ receptor occupancy by the integrin inhibitor GSK3008348 was observed (34). A strength of both the GSK3008348 study and the current PET study is the ability to observe receptor occupancy directly in the affected fibrotic lung tissue of participants with IPF, in contrast to other assay systems such as those using peripheral blood mononuclear cells. While PET has not been widely used to demonstrate receptor occupancy in IPF, both studies support the further use of PET in IPF drug development.

Bexotegrast was also evaluated in the global Phase 2 INTEGRIS-IPF study (NCT04396756) (22). Participants with IPF who received 40, 80, 160, or 320 mg bexotegrast up to 12 weeks experienced a favorable safety and tolerability profile, with no dose relationship for TEAEs observed. Dose-proportional increases in bexotegrast plasma concentrations were observed, which were consistent with the

ANNALSATS Articles in Press. Published November 05, 2024 as 10.1513/AnnalsATS.202409-969OC

current PET results. Analyses in INTEGRIS-IPF—including FVC, quantitative lung fibrosis scores, and circulating levels of fibrosis and IPF progression biomarkers—suggested an antifibrotic effect of bexotegrast treatment.

Limitations of this study include the relatively small sample size of the study, with only 8 participants completing PET imaging after bexotegrast treatment. Although the mean study population was 77.6 years old with relatively well-preserved FVC and DL_{CO}, the $\alpha_v\beta_6$ integrin binding observed here is expected to be generalizable across younger patients and those with worse disease severity. Given the slow kinetics of the [^{18}F]FP-$R_0$1-MG-F2 radiotracer, a longer acquisition time may have been informative and enabled an evaluation of optimal scan duration; however, longer acquisition times may be uncomfortable for participants with IPF. Test-retest studies are needed to confirm the sensitivity of this method for estimating $\alpha_v\beta_6$ receptor occupancy.

In summary, following a single dose of bexotegrast dose- and concentration-dependent $\alpha_v\beta_6$ integrin receptor occupancy was observed by PET over the 60 mg to 320 mg dose range. This effect is consistent with the hypothesis that bexotegrast engages with $\alpha_v\beta_6$ integrin receptors in the lungs. Bexotegrast was well tolerated at the administered doses, with no bexotegrast-related TEAEs or serious TEAEs reported during this study. Overall, this study supports the late-stage evaluation of bexotegrast 160 mg and 320 mg doses in the ongoing Phase 2b/3 BEACON-IPF trial (NCT06097260) in IPF.

ANNALSATS Articles in Press. Published November 05, 2024 as 10.1513/AnnalsATS.202409-969OC

Acknowledgments

The authors would like to thank the patients who volunteered to participate in this study (NCT04072315; PLN-74809-201). The authors also thank Michael Maker, who was an employee of Invicro at the time of this study, for his assistance with the data analysis and Karen Morris, PhD, the Stanford Research Coordinator, for the successful recruitment and enrollment efforts for this study. This study was sponsored by Pliant Therapeutics, Inc. Editorial assistance was provided by Richard Karpowicz, PhD, CMPP, of Nucleus Global, Inc., and was funded by Pliant Therapeutics, Inc.

Data Sharing Statement

Clinical study data access for research use: Pliant Therapeutics, Inc. (“Pliant”) understands and acknowledges the need to share clinical study data with the research community in an open and transparent manner. In furtherance of research efforts, a member of the scientific community may request aggregated deidentified clinical data collected during a clinical study after its public disclosure by Pliant and filing of any related intellectual property protection. To the extent that Pliant has any additional supporting documentation or summary data, it may, at its discretion, also make such information available. Pliant will take into consideration any reasonable request that it receives pertaining to clinical data that has been accepted and published by a journal. Prior to receipt of clinical study data, Pliant and the requesting institution shall enter into an agreement which takes into consideration applicable data privacy laws and the use of the clinical study data for research purposes only. All requests for access to clinical study data must be submitted in writing to scientificcommunications@pliantrx.com.

ANNALSATS Articles in Press. Published November 05, 2024 as 10.1513/AnnalsATS.202409-969OC

Role of the Study Sponsor

This study was sponsored by Pliant Therapeutics, Inc. The study sponsor was involved in the study design, data analysis, and preparation of the manuscript.

Author Disclosures

JM has nothing to disclose. **SJ** has nothing to disclose. **ÉAL, GPC, AC, CNB, MJ, SMT,** and **MD** were employed by Pliant Therapeutics, Inc. and owned stock at the time of this analysis. **BW, HD,** and **RK** have nothing to disclose. **GR** and **GS** were employees of Invicro, who were contracted by Pliant Therapeutics, Inc., to perform data analysis reported in this manuscript. **MW** and **HHG** received research funding from Pliant Therapeutics, Inc.

ANNALSATS Articles in Press. Published November 05, 2024 as 10.1513/AnnalsATS.202409-969OC

REFERENCES

1. Lederer DJ, Martinez FJ. Idiopathic pulmonary fibrosis. *N Engl J Med.* 2018;378(19):1811–1823.

2. Raghu G, Collard HR, Egan JJ, Martinez FJ, Behr J, Brown KK, et al. An official ATS/ERS/JRS/ALAT statement: idiopathic pulmonary fibrosis: evidence-based guidelines for diagnosis and management. *Am J Respir Crit Care Med.* 2011;183(6):788–824.

3. Maher TM, Bendstrup E, Dron L, Langley J, Smith G, Khalid JM, et al. Global incidence and prevalence of idiopathic pulmonary fibrosis. *Respir Res.* 2021;22(1):197.

4. Booth AJ, Hadley R, Cornett AM, Dreffs AA, Matthes SA, Tsui JL, et al. Acellular normal and fibrotic human lung matrices as a culture system for in vitro investigation. *Am J Respir Crit Care Med.* 2012;186(9):866–876.

5. Guo H, Sun J, Zhang S, Nie Y, Zhou S, Zeng Y. Progress in understanding and treating idiopathic pulmonary fibrosis: recent insights and emerging therapies. *Front Pharmacol.* 2023;14:1205948.

6. Raghu G, Chen SY, Yeh WS, Maroni B, Li Q, Lee YC, et al. Idiopathic pulmonary fibrosis in US Medicare beneficiaries aged 65 years and older: incidence, prevalence, and survival, 2001-11. *Lancet Respir Med.* 2014;2(7):566–572.

7. Strongman H, Kausar I, Maher TM. Incidence, prevalence, and survival of patients with idiopathic pulmonary fibrosis in the UK. *Adv Ther.* 2018;35(5):724–736.

8. Saito A, Horie M, Nagase T. TGF-β Signaling in lung health and disease. *Int J Mol Sci.* 2018;19(8). Epub 20180820. doi: 10.3390/ijms19082460.

ANNALSATS Articles in Press. Published November 05, 2024 as 10.1513/AnnalsATS.202409-969OC

9. Henderson NC, Sheppard D. Integrin-mediated regulation of TGFβ in fibrosis. *Biochim Biophys Acta.* 2013;1832(7):891–896.

10. Reed NI, Jo H, Chen C, Tsujino K, Arnold TD, DeGrado WF, et al. The αvβ1 integrin plays a critical in vivo role in tissue fibrosis. *Sci Transl Med.* 2015;7(288):288ra79.

11. Robertson IB, Rifkin DB. Regulation of the bioavailability of TGF-β and TGF-β-related proteins. *Cold Spring Harb Perspect Biol.* 2016;8(6).

12. Decaris ML, Schaub JR, Chen C, Cha J, Lee GG, Rexhepaj M, et al. Dual inhibition of $\alpha_v\beta_6$ and $\alpha_v\beta_1$ reduces fibrogenesis in lung tissue explants from patients with IPF. *Respir Res.* 2021;22(1):265.

13. Munger JS, Huang X, Kawakatsu H, Griffiths MJ, Dalton SL, Wu J, et al. The integrin alpha v beta 6 binds and activates latent TGF beta 1: a mechanism for regulating pulmonary inflammation and fibrosis. *Cell.* 1999;96(3):319–328.

14. Flanders KC. Smad3 as a mediator of the fibrotic response. *Int J Exp Pathol.* 2004;85(2):47–64.

15. Kimura RH, Wang L, Shen B, Huo L, Tummers W, Filipp FV, et al. Evaluation of integrin $\alpha v\beta_6$ cystine knot PET tracers to detect cancer and idiopathic pulmonary fibrosis. *Nat Commun.* 2019;10(1):4673.

16. Horan GS, Wood S, Ona V, Li DJ, Lukashev ME, Weinreb PH, et al. Partial inhibition of integrin alpha(v)beta6 prevents pulmonary fibrosis without exacerbating inflammation. *Am J Respir Crit Care Med.* 2008;177(1):56–65.

17. Saini G, Porte J, Weinreb PH, Violette SM, Wallace WA, McKeever TM, et al. αvβ6 integrin may be a potential prognostic biomarker in interstitial lung disease. *Eur Respir J.* 2015;46(2):486–494.

ANNALSATS Articles in Press. Published November 05, 2024 as 10.1513/AnnalsATS.202409-969OC

18. Bowman WS, Newton CA, Linderholm AL, Neely ML, Pugashetti JV, Kaul B, et al. Proteomic biomarkers of progressive fibrosing interstitial lung disease: a multicentre cohort analysis. *Lancet Respir Med.* 2022;10(6):593–602.

19. Oldham JM, Huang Y, Bose S, Ma SF, Kim JS, Schwab A, et al. Proteomic biomarkers of survival in idiopathic pulmonary fibrosis. *Am J Respir Crit Care Med.* 2024;209(9):1111–1120.

20. Shi N, Wang Z, Zhu H, Liu W, Zhao M, Jiang X, et al. Research progress on drugs targeting the TGF-β signaling pathway in fibrotic diseases. *Immunol Res.* 2022;70(3):276–288.

21. Maher JM, Zhang R, Palanisamy G, Perkins K, Liu L, Brassil P, et al. Lung-restricted ALK5 inhibition avoids systemic toxicities associated with TGFβ pathway inhibition. *Toxicol Appl Pharmacol.* 2022;438:115905.

22. Lancaster L, Cottin V, Ramaswamy M, Wuyts WA, Jenkins RG, Scholand MB, et al. Bexotegrast in patients with idiopathic pulmonary fibrosis: the INTEGRIS-IPF Study. *Am J Respir Crit Care Med.* 2024. Epub 20240606.

23. Mooney JJ, Morris K, Jacobs S, Lefebvre E, Cosgrove GP, Wong S, et al. PLN-74809, a dual-selective inhibitor of integrins αvβ6 and αvβ1, shows dose-dependent target engagement in the lungs of patients with idiopathic pulmonary fibrosis (IPF) (abstract). *Am J Respir Crit Care Med*. 2022;205:A5254.

24. Wardak M, Turner S, Mooney J, Rizzo G, Morris K, Jacobs Su, et al. Phase 2 drug target engagement study of PLN-74809 in patients with idiopathic pulmonary fibrosis using a novel αvβ6 cystine knot PET imaging tracer. *Journal of Nuclear Medicine*. 2022;63(Suppl 2):2236.

ANNALSATS Articles in Press. Published November 05, 2024 as 10.1513/AnnalsATS.202409-969OC

25. Lynch DA, Sverzellati N, Travis WD, Brown KK, Colby TV, Galvin JR, et al. Diagnostic criteria for idiopathic pulmonary fibrosis: a Fleischner Society White Paper. *Lancet Respir Med.* 2018;6(2):138–153.

26. Gunn RN, Slifstein M, Searle GE, Price JC. Quantitative imaging of protein targets in the human brain with PET. *Phys Med Biol.* 2015;60(22):R363–R411.

27. Ofev (nintedanib capsules) [prescribing information]. Ridgefield, CT: Boehringer Ingelheim Pharmaceuticals, Inc, October, 2022.

28. Lancaster L, Crestani B, Hernandez P, Inoue Y, Wachtlin D, Loaiza L, et al. Safety and survival data in patients with idiopathic pulmonary fibrosis treated with nintedanib: pooled data from six clinical trials. *BMJ Open Respir Res.* 2019;6(1):e000397.

29. Nathan SD, Albera C, Bradford WZ, Costabel U, Glaspole I, Glassberg MK, et al. Effect of pirfenidone on mortality: pooled analyses and meta-analyses of clinical trials in idiopathic pulmonary fibrosis. *Lancet Respir Med.* 2017;5(1):33–41.

30. King TE, Bradford WZ, Castro-Bernardini S, Fagan EA, Glaspole I, Glassberg MK, et al. A phase 3 trial of pirfenidone in patients with idiopathic pulmonary fibrosis. *N Engl J Med.* 2014;370(22):2083–2092.

31. Petnak T, Lertjitbanjong P, Thongprayoon C, Moua T. Impact of antifibrotic therapy on mortality and acute exacerbation in idiopathic pulmonary fibrosis: a systematic review and meta-analysis. *Chest.* 2021;160(5):1751–1763.

32. Richeldi L, du Bois RM, Raghu G, Azuma A, Brown KK, Costabel U, et al. Efficacy and safety of nintedanib in idiopathic pulmonary fibrosis. *N Engl J Med.* 2014;370(22):2071–2082.

ANNALSATS Articles in Press. Published November 05, 2024 as 10.1513/AnnalsATS.202409-969OC

33. Levra S, Guida G, Sprio AE, Crosa F, Ghio PC, Bertolini F, et al. Long-term safety of antifibrotic drugs in IPF: a real-world experience. *Biomedicines.* 2022;10(12).

34. Maher TM, Simpson JK, Porter JC, Wilson FJ, Chan R, Eames R, et al. A positron emission tomography imaging study to confirm target engagement in the lungs of patients with idiopathic pulmonary fibrosis following a single dose of a novel inhaled αvβ6 integrin inhibitor. *Respir Res.* 2020;21(1):75.

ANNALSATS Articles in Press. Published November 05, 2024 as 10.1513/AnnalsATS.202409-969OC

Figure Legends

Figure 1. Study design.*

CT, computed tomography; EOS, end of study; PET, positron emission tomography.

*Participants could elect to receive a second, different dose of bexotegrast after a 14-day bexotegrast washout period. For these participants, safety was evaluated through 7 days after their second round of dosing and PET/CT imaging.

Figure 2. Participant disposition**.**

AE, adverse event; ITT, intention to treat; mITT, modified intention to treat; PET, positron emission tomography; PK, pharmacokinetic.

*Due to sponsor's decision to postpone the study.

Figure 3. Arithmetic mean (**A**) total and (**B**) unbound plasma bexotegrast concentration versus time profiles following single oral doses of 60 to 320 mg bexotegrast (PK concentration population) (semi-logarithmic scale).

PK, pharmacokinetic.

Figure 4. V_T values in the lung25 ROI, plotted against dose of bexotegrast (mITT population).

Lung25, the top 25th percentile of lung signal at 60 minutes; mITT, modified intention to treat; ROI, region of interest; V_T, PET volume of distribution.

Figure 5. Plot of V_T in the lung25 ROI against unbound plasma concentration of bexotegrast, together with a model fit using Equation 2 (mITT population).

Lung25, the top 25th percentile of lung signal at 60 minutes; mITT, modified intention to treat; ROI, region of interest; V_T, PET volume of distribution.

ANNALSATS Articles in Press. Published November 05, 2024 as 10.1513/AnnalsATS.202409-969OC

Figure 6. Predicted peak effect following single doses of bexotegrast, based on the dose-PK data and the model of Equation 4* (mITT population).
C_{max}, maximum observed concentration; ITT, modified intention to treat; PET, positron emission tomography; PK, pharmacokinetic; ub, unbound bexotegrast.
*Bexotegrast PK data from all participants enrolled in the study were used to estimate the mean C_{max}.

Figure 7. Knottin PET images of the lungs in coronal, axial, and sagittal projections at baseline (**A**) and post-treatment with a 320-mg dose of bexotegrast (**B**) demonstrating decreased tracer uptake by lungs after drug treatment, consistent with integrin $\alpha_v\beta_6$ binding by bexotegrast and competitive inhibition of knottin tracer binding post treatment.
PET, positron emission tomography.

ANNALSATS Articles in Press. Published November 05, 2024 as 10.1513/AnnalsATS.202409-969OC

Table 1. Baseline Demographics and Disease Characteristics (Safety Population)

Characteristic	Pooled Bexotegrast (n=9)
Age, mean (SD), years	77.6 (4.4)
Male sex, n (%)	7 (77.8)
Female sex, n (%)	2 (22.2)
Race, n (%)	
White	8 (88.9)
Native Hawaiian or Other Pacific Islander	1 (11.1)
Weight, mean (SD), kg	74.6 (13.1)
BMI, mean (SD), kg/m^2	25.2 (2.47)
FVC	
Mean (SD), mL	2967.8 (829.3)
Percent predicted, mean (SD)	83.7 (17.7)
FEV1	
Mean (SD), mL	2370.0 (554.3)
Percent predicted, mean (SD)	98.9 (21.9)
FEV1/FVC, mean (SD)	0.81 (0.07)
DL_{CO}	
Mean (SD), mL/mmHg/min	13.9 (4.8)
Adjusted percent predicted, mean (SD)	63.1 (17.9)
GAP index stage, n (%)	

ANNALSATS Articles in Press. Published November 05, 2024 as 10.1513/AnnalsATS.202409-969OC

Stage I	5 (55.6)
Stage II	3 (33.3)
Stage III	1 (11.1)
Time since IPF diagnosis, mean (SD), months	43.8 (18.5)
Concomitant standard of care treatment, n (%)*	
Nintedanib	7 (77.8)
Pirfenidone	1 (11.1)

BMI, body mass index; DLco, diffusing capacity for carbon monoxide; FEV1, forced expiratory volume 1 second; FVC, forced vital capacity, GAP, gender-age-physiology, IPF, idiopathic pulmonary fibrosis.

* Concomitant medications are those ongoing at the date and time of first dose of study drug. Participants are counted once within each drug class and once for each unique preferred name.

ANNALSATS Articles in Press. Published November 05, 2024 as 10.1513/AnnalsATS.202409-969OC

Table 2. Model Fit Parameters Estimated by Fitting Equation 2 to the PK and V_T data (mITT population)

ROI	Fitted model parameters		
	EC_{50} (ng/mL)	V_{ND} (mL/cm^3)	V_S (mL/cm^3)
Lung25	3.32	0.86	1.56
Whole lungs	3.36	0.54	0.87

EC_{50}, half maximal effective concentration; lung25, the top 25th percentile of lung signal at 60 minutes; mITT, modified intention to treat; PK, pharmacokinetic; ROI, region of interest; V_{ND}, non-displaceable volume of distribution; V_s, specific volume of distribution; V_T, PET volume of distribution.

ANNALSATS Articles in Press. Published November 05, 2024 as 10.1513/AnnalsATS.202409-969OC

FIGURES

Figure 1. Study design.*

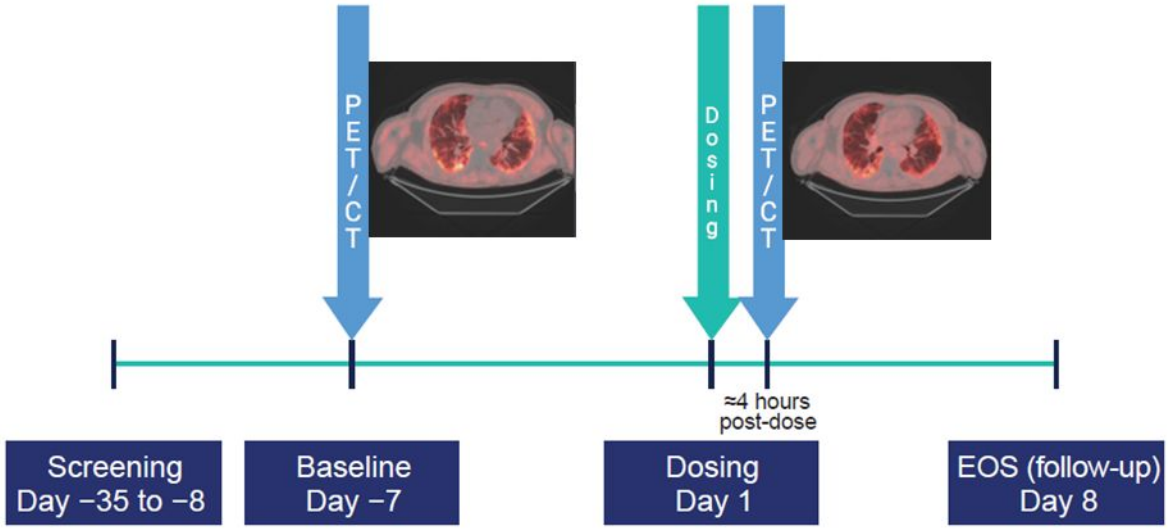

CT, computed tomography; EOS, end of study; PET, positron emission tomography.

*Participants could elect to receive a second, different dose of bexotegrast after a 14-day bexotegrast washout period. For these participants, safety was evaluated through 7 days after their second round of dosing and PET/CT imaging.

ANNALSATS Articles in Press. Published November 05, 2024 as 10.1513/AnnalsATS.202409-969OC

Figure 2. Participant disposition.

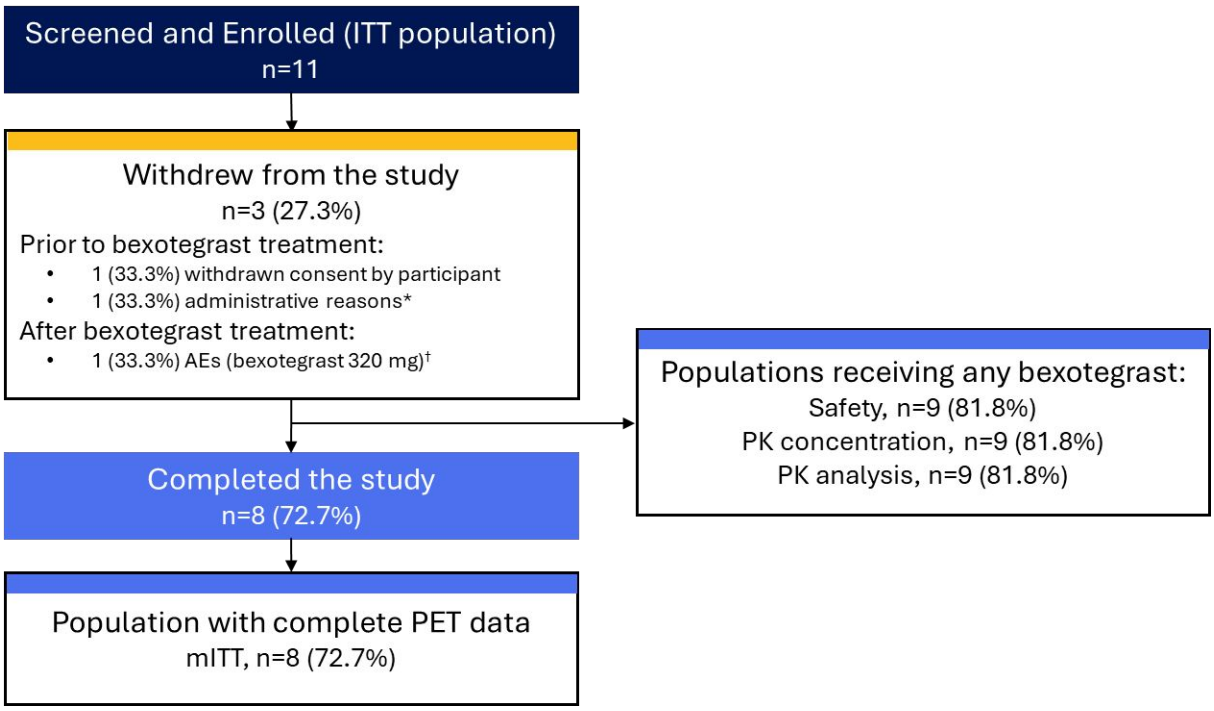

AE, adverse event; ITT, intention to treat; mITT, modified intention to treat; PET, positron emission tomography; PK, pharmacokinetic.

*Due to sponsor's decision to postpone the study.

†One participant who received bexotegrast 320 mg experienced moderate (Grade 2) TEAEs of hepatic enzyme increase and gamma-glutamyl transferase increase on Day 2 that led to withdrawal from the study on Day 8 and were deemed not related to the study drug. The participant had a medical history of hyperbilirubinemia and was concomitantly receiving nintedanib for treatment of IPF.

ANNALSATS Articles in Press. Published November 05, 2024 as 10.1513/AnnalsATS.202409-969OC

Figure 3. Arithmetic mean (**A**) total and (**B**) unbound plasma bexotegrast concentration versus time profiles following single oral doses of 60 to 320 mg bexotegrast (PK concentration population) (semi-logarithmic scale).

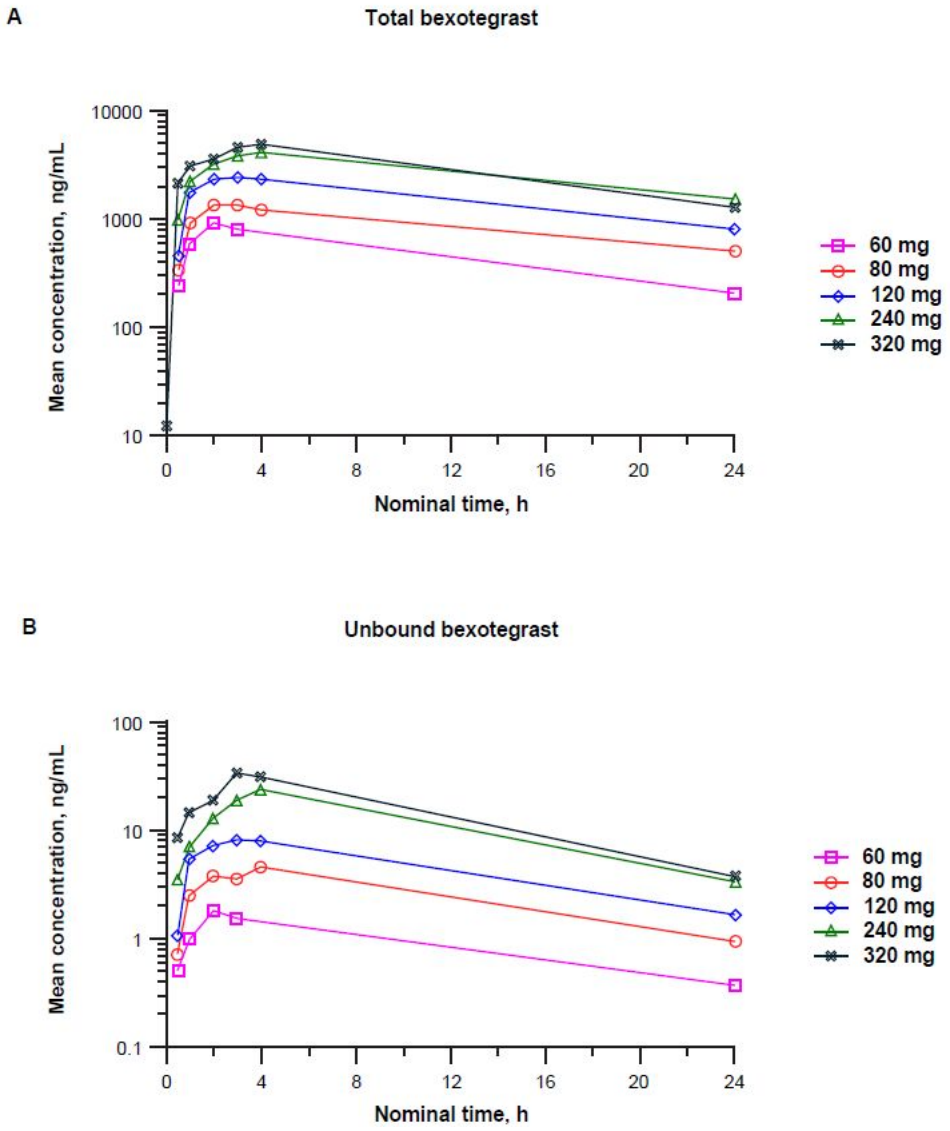

PK, pharmacokinetic.

ANNALSATS Articles in Press. Published November 05, 2024 as 10.1513/AnnalsATS.202409-969OC

Figure 4. V_T values in the lung25 ROI, plotted against dose of bexotegrast (mITT population).

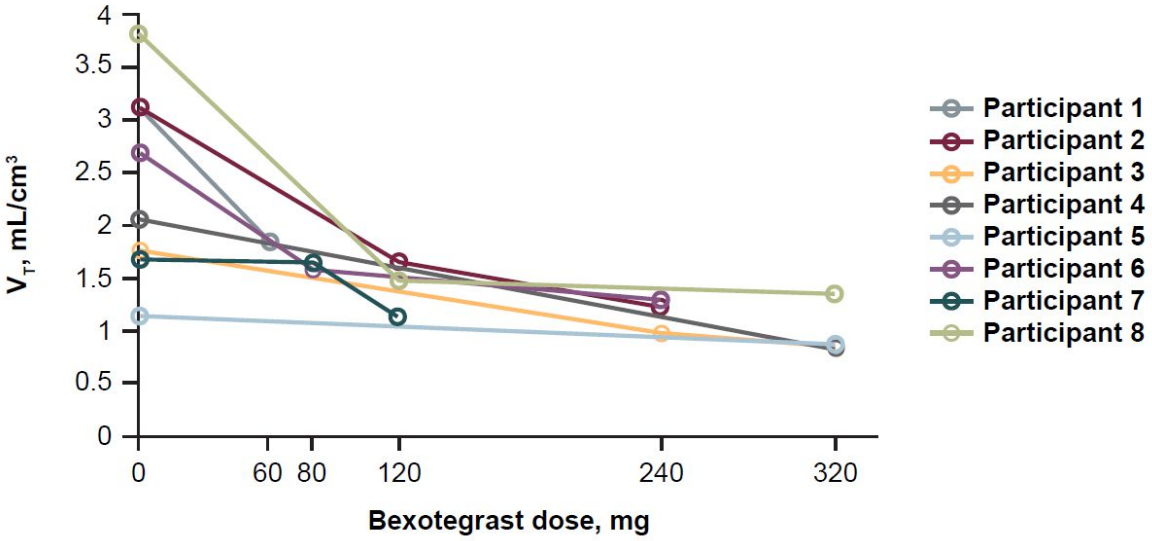

Lung25, the top 25th percentile of lung signal at 60 minutes; mITT, modified intention to treat; ROI, region of interest; V_T, PET volume of distribution.

ANNALSATS Articles in Press. Published November 05, 2024 as 10.1513/AnnalsATS.202409-969OC

Figure 5. Plot of V_T in the lung25 ROI against unbound plasma concentration of bexotegrast, together with a model fit using Equation 2 (mITT population).

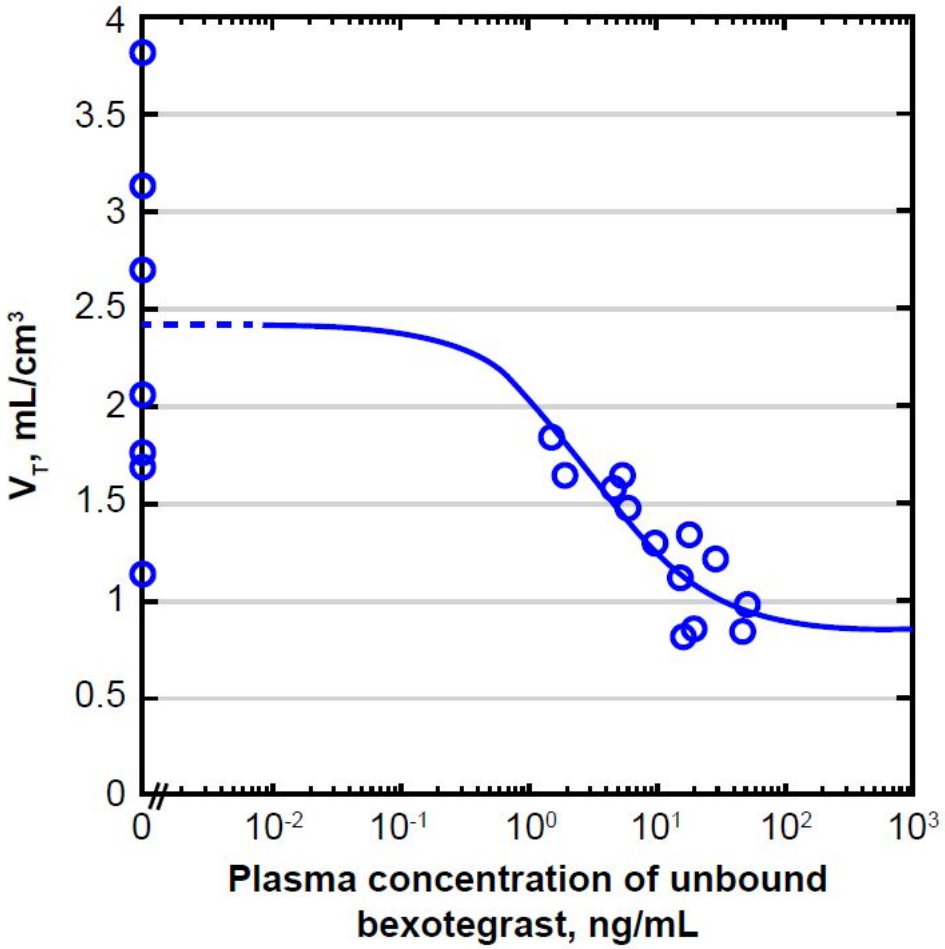

Lung25, the top 25th percentile of lung signal at 60 minutes; mITT, modified intention to treat; ROI, region of interest; V_T, PET volume of distribution.

ANNALSATS Articles in Press. Published November 05, 2024 as 10.1513/AnnalsATS.202409-969OC

Figure 6. Predicted peak effect following single doses of bexotegrast, based on the dose-mean unbound C_{max} data and the model of Equation 4* (mITT population).

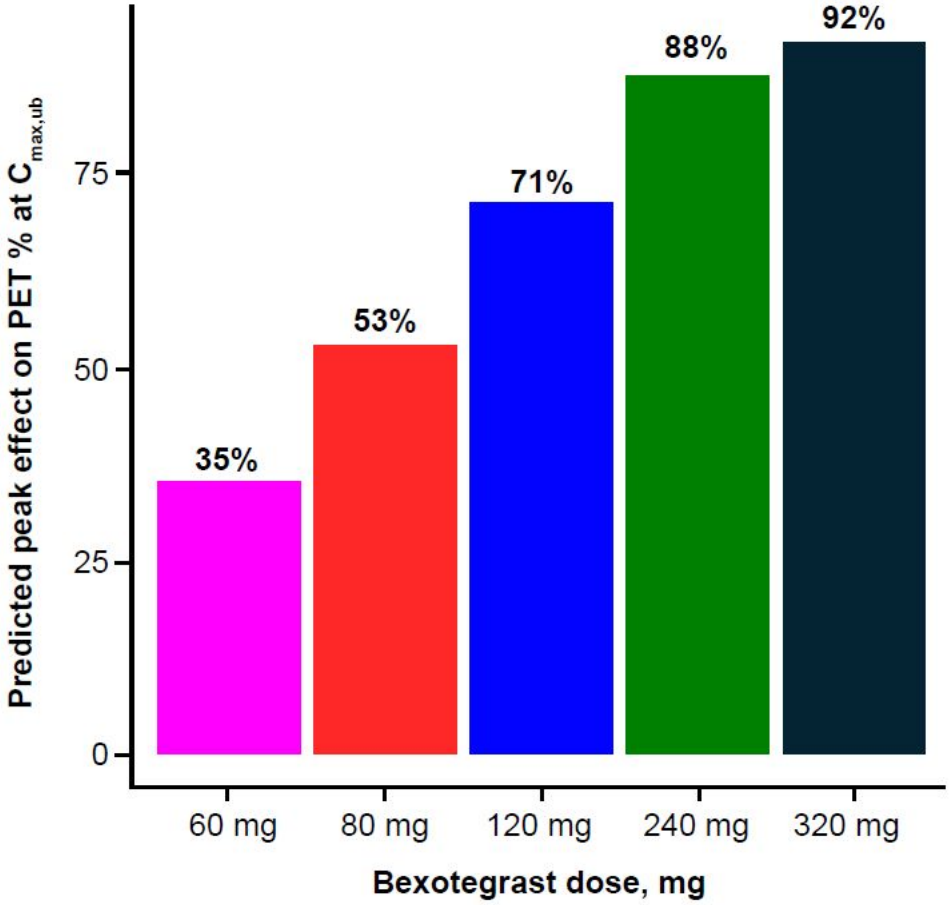

C_{max}, maximum observed concentration; ITT, modified intention to treat; PET, positron emission tomography; PK, pharmacokinetic; ub, unbound bexotegrast.

*Bexotegrast PK data from all participants enrolled in the study were used to estimate the mean unbound C_{max}.

ANNALSATS Articles in Press. Published November 05, 2024 as 10.1513/AnnalsATS.202409-969OC

Figure 7. Knottin PET images of the lungs in coronal, axial, and sagittal projections at baseline (**A**) and post-treatment with a 320-mg dose of bexotegrast (**B**) demonstrating decreased tracer uptake by lungs after drug treatment, consistent with integrin $\alpha_v\beta_6$ binding by bexotegrast and competitive inhibition of knottin tracer binding post treatment.

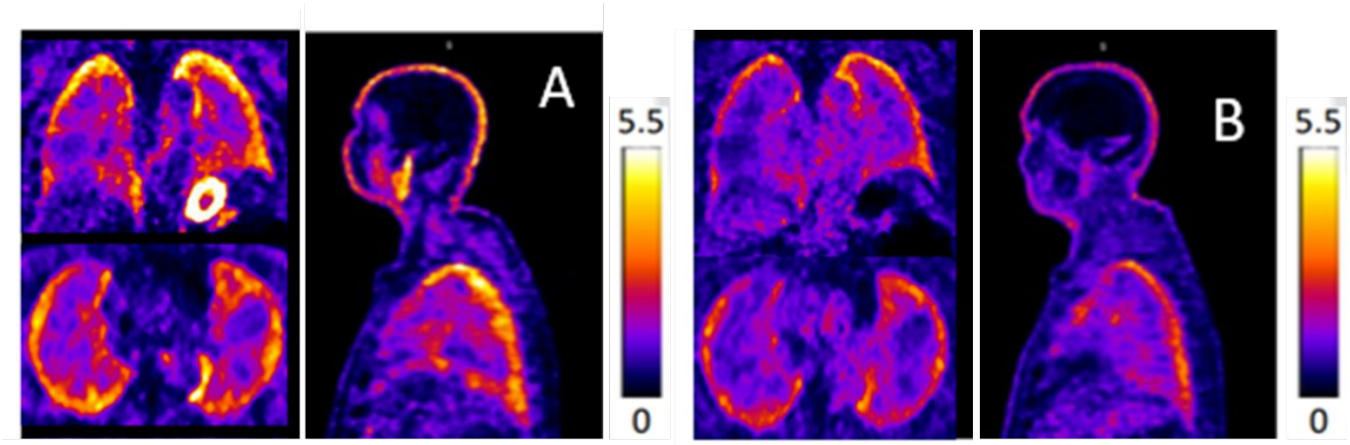

PET, positron emission tomography.

ANNALSATS Articles in Press. Published November 05, 2024 as 10.1513/AnnalsATS.202409-969OC

Bexotegrast Shows Dose-dependent Integrin $\alpha_v\beta_6$ Receptor Occupancy in Lungs of Participants with Idiopathic Pulmonary Fibrosis: A Phase 2, Open-Label Clinical Trial

Joshua J. Mooney, Susan Jacobs, Éric A. Lefebvre, Gregory P. Cosgrove, Annie Clark, Scott Turner, Martin Decaris, Chris N. Barnes, Marzena Jurek, Brittney Williams, Heying Duan, Richard Kimura, Gaia Rizzo, Graham Searle, Mirwais Wardak, H. Henry Guo

Online Data Supplement

ANNALSATS Articles in Press. Published November 05, 2024 as 10.1513/AnnalsATS.202409-969OC

Supplementary Methods

Pharmacokinetic Assessments

Plasma samples for pharmacokinetic (PK) analysis of bexotegrast were obtained before dosing and at 0.5, 1, 2, 3, and 4 hours after dosing on Day 1, prior to receiving the PET tracer, and at 24 hours after dosing (Day 2). The percent unbound bexotegrast was also determined at 0.5, 1, 2, 3, and 4, and 24 hours after dosing on Day 1. Unbound plasma bexotegrast concentrations were calculated as percent unbound × total plasma concentration at each timepoint. For presentation of the individual data and summary statistics, concentrations below the limit of quantitation were set to zero. Blood samples for radiotracer PK were also obtained at 1, 3, 5, 10, 30, and 60 minutes after completion of radiotracer injection for PET to obtain blood time-activity measurements.

Concentration-time data for bexotegrast in plasma were analyzed using noncompartmental methods in Phoenix® WinNonlin® (Version 8.3.4, Certara, LP) in conjunction with Certara IntegralTM (Version 22.10.1, Certara, LP). During the PK analysis, below the limit of quantitation (BLQ) concentrations up to the time of the first quantifiable concentration were treated as zero. Embedded (values between 2 quantifiable concentrations) and terminal BLQ concentrations were treated as “missing.” PK analyses were performed using actual time relative to dosing.

ANNALSATS Articles in Press. Published November 05, 2024 as 10.1513/AnnalsATS.202409-969OC

Supplementary Table

Table E1. Descriptive Statistics for Unbound Plasma Bexotegrast Pharmacokinetic Parameters Following Single Doses of 60 to 320 mg Bexotegrast (PK Analysis Population)

Parameter, mean (SD) [n]	Bexotegrast 60 mg	Bexotegrast 80 mg	Bexotegrast 120 mg	Bexotegrast 240 mg	Bexotegrast 320 mg
$C_{max,u}$ (ng/mL)	1.8 (NC) [1]	3.8 (2.6) [2]	8.3 (5.1) [4]	24.2 (20.1) [4]	40.5 (29.9) [5]
$AUC_{0-24,u}$ (h×ng/mL)	20.6 (NC) [1]	48.0 (20.2) [2]	103 (65.6) [4]	208 (186) [2]	429 (195) [3]

AUC, area under the curve; $C_{max,u}$, maximum unbound plasma concentration; NC, not calculated; PK, pharmacokinetic.

ANNALSATS Articles in Press. Published November 05, 2024 as 10.1513/AnnalsATS.202409-969OC

Table E2. Safety Profile of Bexotegrast (Safety Population)

Participants with TEAEs, n (%)	Bexotegrast 60 mg (n = 1)	Bexotegrast 80 mg (n = 2)	Bexotegrast 120 mg (n = 4)	Bexotegrast 240 mg (n = 4)	Bexotegrast 320 mg (n = 5)	Overall (n=9)
Any TEAE	0	0	0	0	1 (20.0)	1 (11.1)
Any study drug-related TEAE	0	0	0	0	0	0
Any procedure-related TEAE	0	0	0	0	0	0
Any serious TEAE	0	0	0	0	0	0
Any TEAE leading to study withdrawal	0	0	0	0	1 (20.0)	1 (11.1)

ANNALSATS Articles in Press. Published November 05, 2024 as 10.1513/AnnalsATS.202409-969OC

Any TEAE leading to death	0	0	0	0	0	0

TEAE, treatment-emergent adverse event.

ANNALSATS Articles in Press. Published November 05, 2024 as 10.1513/AnnalsATS.202409-969OC

Supplementary Figures

Figure E1. Baseline coronal PET/CT images of the lungs of a representative participant demonstrating heterogeneously increased $\alpha_v\beta_6$ integrin cystine knot peptide radiotracer (knottin) binding in areas of fibrosis in participants with IPF, including: (**A**) a representative maximal intensity projection PET/CT image, (**B**) a representative coronal plane CT image, (**C**) the corresponding PET image, and (**D**) PET/CT overlay showing increased radiotracer uptake in areas of reticulation and traction bronchiectasis/bronchiolectasis with apical to basilar gradient.

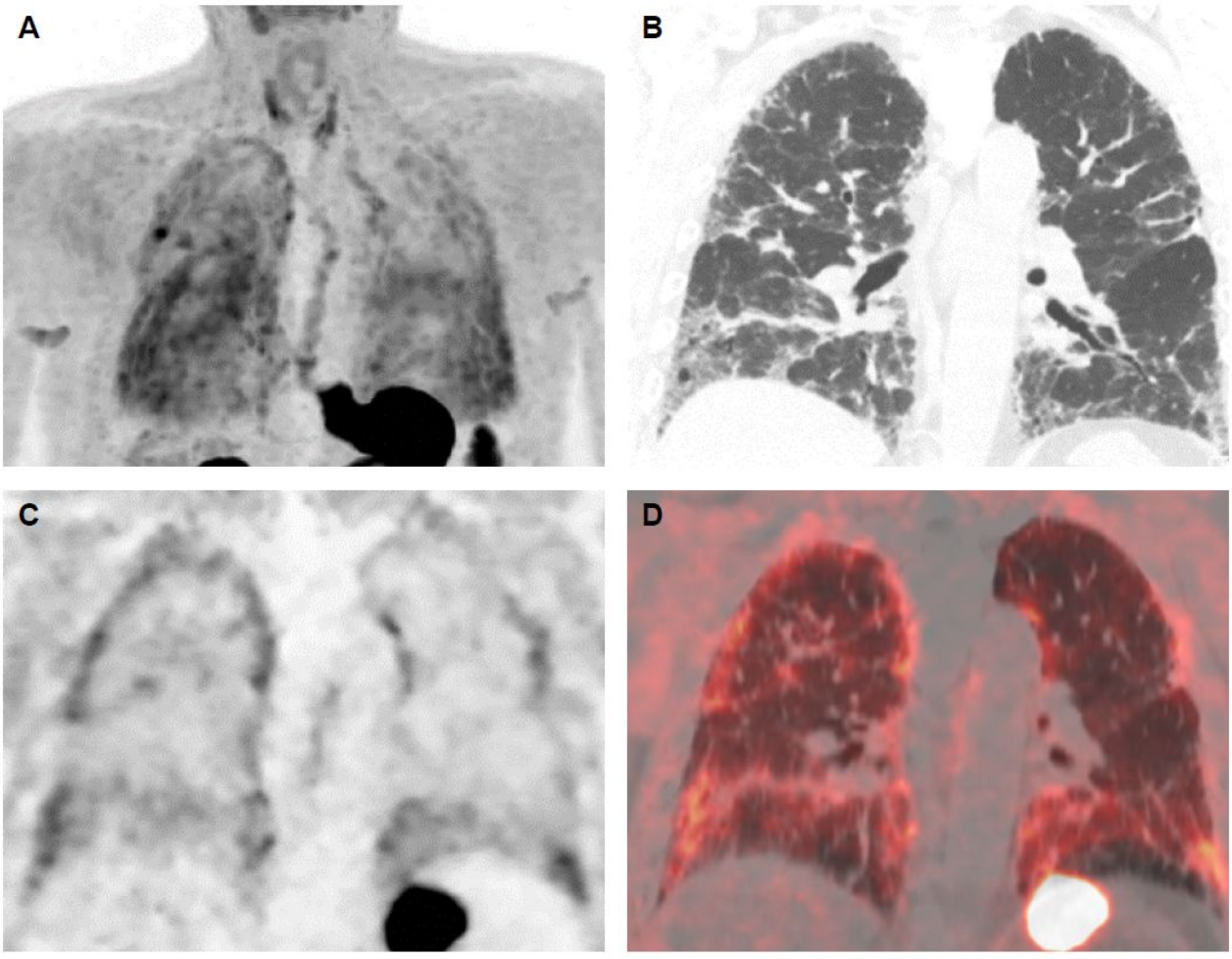

CT, computed tomography; IPF, idiopathic pulmonary fibrosis; PET, positron emission tomography.

ANNALSATS Articles in Press. Published November 05, 2024 as 10.1513/AnnalsATS.202409-969OC

Figure E2. Regional tissue TACs for representative participant: (**A**) baseline scan, (**B**) scan following 240-mg dose of bexotegrast, and (**C**) scan following 320-mg dose of bexotegrast.

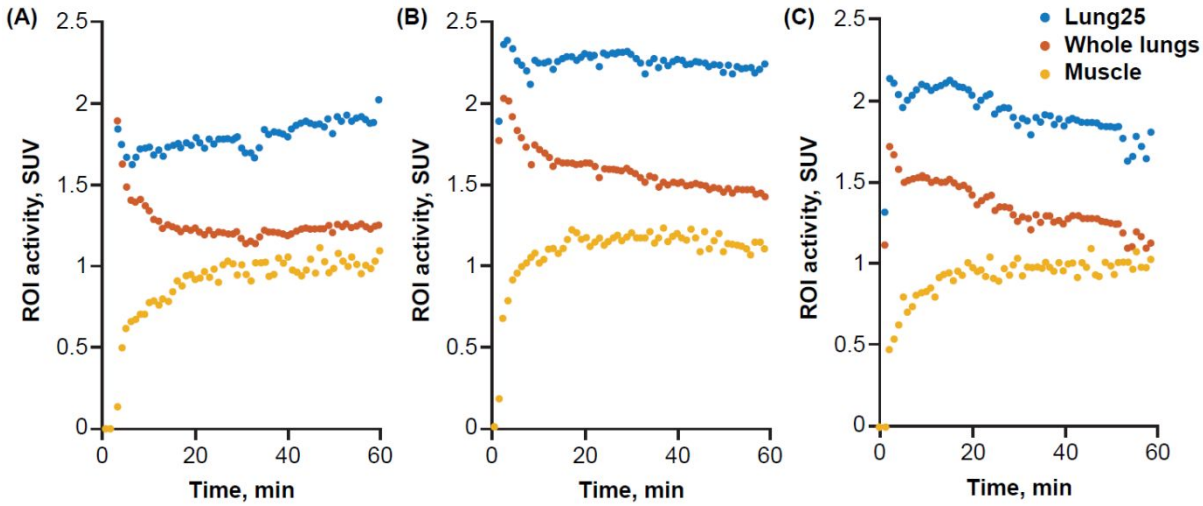

lung25, the top 25th percentile of lung signal at 60 minutes; ROI, region of interest; TAC, time-activity curve.

ANNALSATS Articles in Press. Published November 05, 2024 as 10.1513/AnnalsATS.202409-969OC

Figure E3. Kinetic model fits (1TC model) to regional tissue TACs for a representative participant: (**A**) baseline scan, (**B**) scan following 240-mg dose of bexotegrast and (**C**) scan following 320-mg dose of bexotegrast.

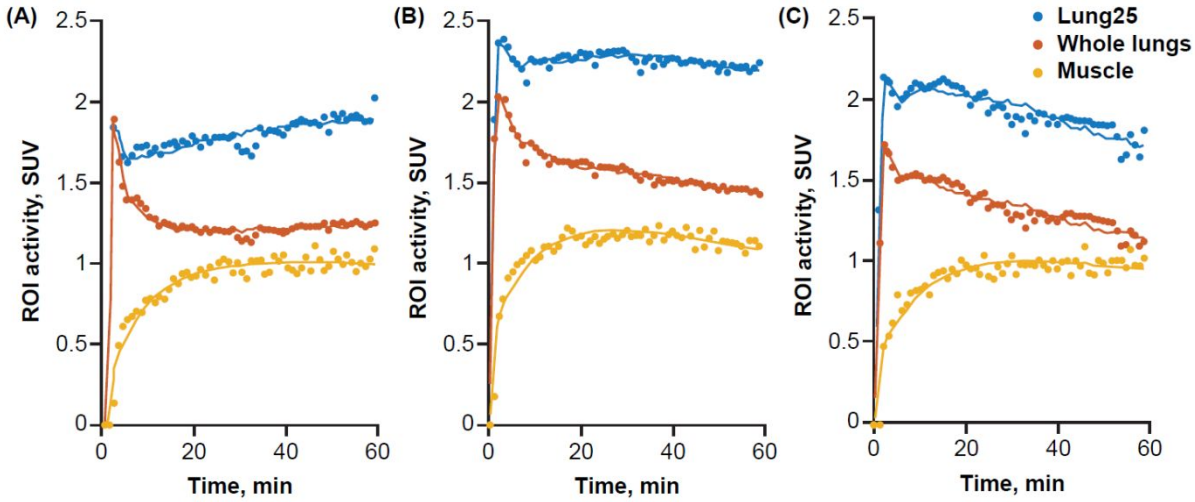

1TC, 1-tissue compartment; lung25, the top 25th percentile of lung signal at 60 minutes; ROI, region of interest; TAC, time-activity curve.

ANNALSATS Articles in Press. Published November 05, 2024 as 10.1513/AnnalsATS.202409-969OC